



Satellite structure in Auger and ($e, 2e$) spectra of germanium

M.R. Went^{*}, M. Vos, A.S. Kheifets

Atomic and Molecular Physics Laboratory, Research School of Physical Sciences and Engineering, The Australian National University, Canberra, 0200 Australia

Abstract

The interpretation of electron spectroscopy data is often complicated by the presence of satellites. These satellites are either due to different final states reached after the excitation (intrinsic satellites) or due to energy loss experienced by the escaping electron on its way out the target (extrinsic satellites). Unravelling these two contributions in an unambiguous way is difficult. In this paper we compare the intrinsic satellite structures obtained for germanium by two different high-energy spectroscopies: Auger spectroscopy of deep core levels and valence band electron momentum spectroscopy. Despite the different nature of the two probes we find a similar shape of the intrinsic satellites and comparable intensity.

© 2006 Elsevier Ltd. All rights reserved.

PACS: 79.20.Fv; 71.20.Mq; 79.20.Kz; 61.43.Dq

Keywords: Germanium; Electron momentum spectroscopy; Auger electron spectroscopy

1. Introduction

Recent measurements of KLL Auger spectra of transition metals have shown that there are, besides the multiplet structure, additional peaks present in the spectra (Kövrer et al., 1999; Kovalík et al., 2002; Berényi et al., 2004; Went and Vos, 2005). Part of these structures are due to inelastic energy losses of the escaping electrons. Electron energy loss spectroscopy (EELS) can be used to study these extrinsic energy loss processes. EELS spectra of germanium show a well-defined peak near 16 eV energy loss (see e.g. Zeppenfeld and Raether, 1966). These extrinsic loss processes shift intensity of the Auger spectra to lower kinetic energy.

A simple technique (Tougaard, 1988) exists for removal of these contributions. However, after removal of the extrinsic loss intensity the Auger spectra still reveal more peaks than is expected based on its multiplet structure alone.

It has been proposed that these additional satellites may be due to 'shake' effects where electrons are excited within the atom as it is ionised from a $3d_{5/2}$ to $4d_{5/2}$ level (Berényi et al., 2004). These shake satellites appear at lower energies separated from the parent transition by a fixed energy. Alternatively, all or some of this intensity can be attributed to intrinsic plasmons. Similar effects are known to occur in electron momentum spectroscopy (EMS, also referred to as ($e, 2e$) spectroscopy). For example, intrinsic satellites were identified in the case of Al (Vos et al., 2002) and Si (Kheifets et al., 2003). Here we want to compare the satellite structure for the case of germanium as observed by inner shell Auger transitions and by EMS of the valence band. If the satellites have, in both cases, a similar origin we would expect this to be

^{*}Corresponding author. Tel.: +61 2 6125 2705; fax: +61 2 6125 2452.

E-mail address: michael.went@anu.edu.au (M.R. Went).

URL: <http://www.rpsphysse.anu.edu.au/ampl/research/ems/index.html>.

reflected in their shape and possibly their relative intensity. Note, however, that there are also distinct differences between both techniques. In particular, the final state of the KLL Auger process contains two core holes, whereas the final state of the EMS measurement contains a single hole in the valence band. In spite of this, our results indicate that the satellite structure in the Auger and EMS spectra have a similar shape and relative intensity of the same order of magnitude. Thus, Auger and EMS results corroborate each other indicating a similar origin for both satellite structures.

2. Experiment

The use of the spectrometer for EMS experiments is described in detail (Vos et al., 2000), its application for high-energy Auger spectroscopy is described in Went and Vos (2005). Amorphous Ge samples are prepared by evaporation of sintered lumps of Ge via resistive heating in a tantalum boat. Approximately 100 nm of Ge is deposited onto free-standing 3 nm thick carbon films. The thickness of the deposited films is monitored by a quartz crystal thickness monitor. The use of thin free-standing carbon/germanium films as a target ensures that the length of the trajectories of the electrons involved in the experiment are small. As we will see, this implies that the probability of extrinsic plasmon excitations is small and makes the subtraction of this contribution straightforward.

Samples are transferred under vacuum into the spectrometer. Here an electron gun produces a well collimated 25 keV electron beam which is incident on one of the samples from the carbon film side. For an Auger measurement the sample and the high voltage sphere in which it is contained is held near 8.5 kV, meaning that 33.5 keV electrons are incident on the sample. In this way the analyser, detecting the ≈ 8.5 keV Ge KLL Auger electrons, can be operated conveniently close to ground. Two hemispherical energy analysers are positioned at $\pm 44.3^\circ$ relative to the incident beam direction. For an EMS measurement the sample and sphere are held at +25 keV and thus 50 keV electrons impinge on the sample and scattered and ejected electrons with an energy near 25 keV are detected *in coincidence* in two separate analysers. In both experiments most of the beam passes through the sample and is collected in a Faraday cup.

The spectrometers collect electrons on a section of a cone with an azimuthal range of $\approx 13^\circ$ which are dispersed through the spectrometer and detected on a position sensitive detector. Thus, the energy and azimuthal angle (within the accepted range; 80 eV and $\pm 6.5^\circ$, respectively) of each electron detected is mapped independently onto the detector plate.

Typically, the measurements take several days. During this time the vacuum in the main chamber is maintained better than 2×10^{-10} torr ensuring that sample quality is maintained. The energy resolution of the Auger experiment is typically 1 eV which is derived from the intrinsic resolution of the analyser (0.6 eV), and a high frequency ripple on the high voltage power supplies (0.1 eV) and a typical drift over a measurement period (0.3 eV). For the EMS measurements the drift and ripple of the target is compensated for by changing the gun voltage and hence should not contribute to the overall resolution (Vos et al., 2000). However, in this experiment, the energy spread of the incoming beam and the energy resolution of *two* analysers come into play, resulting again into an overall energy resolution near 1 eV.

3. Results and discussion

In Fig. 1 we present the $KL_{23}L_{23}$ Auger spectrum of Ge after we subtracted an energy-independent background. In the Auger spectrum we can identify four peaks that appear at positions in reasonable agreement with calculated multiplet splitting (Larkins, 1977) and an additional peak 16 eV below the main 1D_2 component. Part, or all of this, could be due to extrinsic energy losses of the escaping electrons.

In order to investigate this we lowered the energy of the electron hitting the target to 8.5 keV and measured an EELS spectrum in our detector (see Fig. 1 (insert)). These electrons have to transverse the complete film with thickness t . As the detector is positioned at 44.3° relative to the incoming beam the average path length for each transmitted electron is $1.2t$. For Auger electrons the thickness that must be travelled by an electron varies from $\sqrt{2}t$ (Auger electron originating from entrance side) to 0 (Auger electron originating from exit side) so on average the Auger electron must travel $\approx 0.7t$ (Fig. 2). Here we assume that the electron path is basically straight as the probability that an energetic electron is deflected over a significant angle in such a thin film is small. Thus, the intensity due to extrinsic losses is $0.7t/1.2t \approx 0.6$ times smaller than in the EELS spectrum. Using this number and the measured EELS spectrum we can subtract the background due to extrinsic energy losses from the raw Auger data. This 'background subtracted' spectrum is shown as well in Fig. 1.

In EMS the real momentum of electrons in the sample are measured. Unlike other methods that require single crystals to measure dispersion, EMS works equally well for amorphous and polycrystalline targets as it does for single crystal. An EMS measurement of a polycrystalline sample should correspond to the spherically averaged result of a calculation for a single crystal. The same

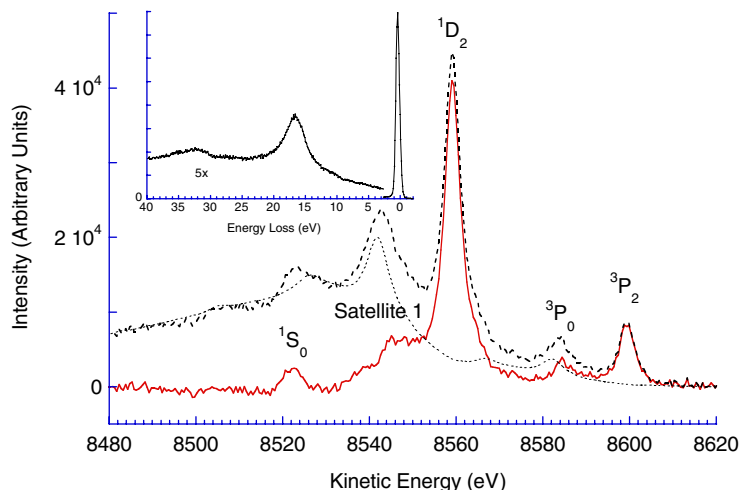


Fig. 1. Ge KLL Auger spectra. The figure shows the raw spectrum (dashed line), background removed spectrum (thick solid line), the background intensity (dotted line). The 8.5 keV EELS spectrum is shown as an insert.

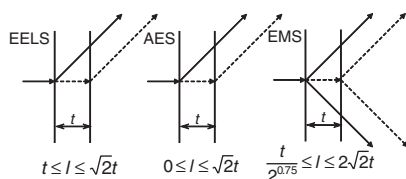


Fig. 2. Schematic diagram showing the path lengths l of electrons through a thin film for an EELS, Auger and EMS experiment.

spherically averaged theory is usually used as a starting point for the interpretation of the spectra of an amorphous film.

Fig. 3 shows the EMS results for amorphous Ge for both raw and deconvoluted data. Inelastic scattering also causes a background in EMS. A deconvolution procedure similar to that used for the Auger spectrum is used to remove this background. First, an EELS measurement of the Ge film is measured at 25 keV electron energy. For an electron produced in a $(e, 2e)$ event at the incoming side of the film, the thickness is $2\sqrt{2}t$ (sum of the paths for the two outgoing electrons, see Fig. 2). For an $(e, 2e)$ event produced at the exit of the film we must consider that the film is traversed now at 50 keV. The mean free path between inelastic collisions is of the order of $E^{0.75}$ (Tanuma et al., 1993). Thus, the effective path length is close to $t/2^{0.75}$. On average, the path length for EMS is then $\approx 1.7t$. As for the 8.5 keV EELS the average path length for these EELS electrons is $1.2t$. Therefore the film appears thicker in a EMS experiment in comparison to an EELS experiment by a factor of $1.7t/1.2t \approx 1.4$. Using this value and the EELS measurement at 25 keV, the background due to inelastic scattering can be removed

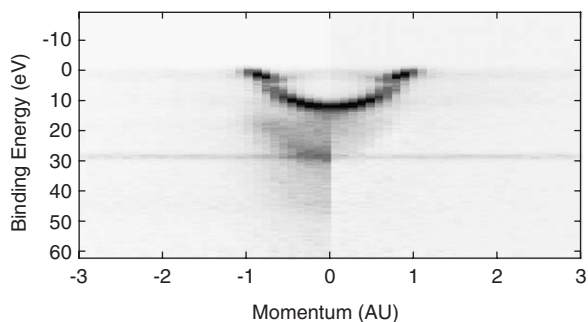


Fig. 3. EMS spectra prior to (left) and after (right) the deconvolution procedure. Intense core level is visible near 30 eV binding energy.

from the EMS measurement. This spectra is presented in the right-half of Fig. 3. The raw and deconvoluted spectra is also presented in Fig. 4 for momentum intervals as indicated.

Examining more closely Fig. 3 we see that the valence band is split. The lower part is an intense parabola-like structure with maximum binding energy at zero momentum. As this feature extends out towards higher momentum it tapers off giving a band width of ≈ 6 eV for the inner valence band. A small band gap separates this and another band which is visible near the fermi level. The maximum intensity of this band is around 3 eV binding energy, 0.7 au. In the left panel of Fig. 3 (raw spectra) we see a broad copy of the valence band ≈ 16 eV lower in energy caused by the well defined peaks in the inelastic scattering. In the right part of the figure this has been removed by the deconvolution procedure described. Also visible in the grey-scale plot is the weak 3d core level (near 29 eV binding energy) which

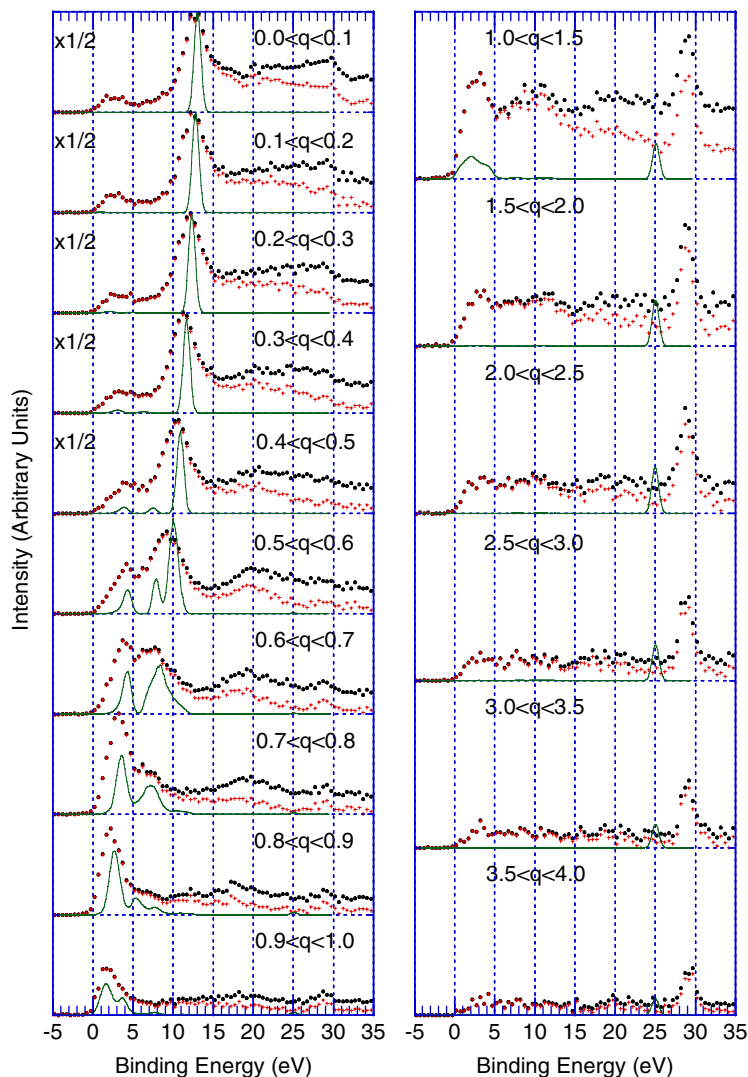


Fig. 4. EMS spectra for 0.1 au (left), 0.5 au (right) momentum spacings. Circles (black online) represent the raw data, the crosses (red online) represent data that has been deconvoluted while the line (green online) represents a LMTO calculation (scaled where indicated).

extends over a large momentum range. Its intensity is weak at low momentum values and here its intensity is partially obscured by inelastic scattering contribution of the valence band. As the 3d core electrons are localised near the nucleus of Ge, they extend, as a consequence of the Heisenberg uncertainty principle over a wide range in momentum space. No dispersion of the 3d level could be detected.

The energy plots in Fig. 4 show more clearly the dispersion. In particular, we can see a definite band gap at 5 eV despite this being an amorphous sample. This is contrary to what was seen with amorphous Si (Bowles et al., 2006), where the band gap was not observed. In Si the gap only became visible when single crystal samples were examined. We also present linear muffin-tin orbital

(LMTO) calculations for the spectral momentum density of Ge. These calculations, treating the 3d electrons as valence electrons, have been spherically average and convoluted with our experimental resolution to aid in comparison. Overall, the theory describes the observations, accurately determining the dispersion of the bands. At low momentum we present the theory scaled to the experiment at zero momentum, while the agreement in position is good the intensity is poor this is most likely due to life-time broadening in the measurements which has not been included in the theory. In the right-hand side of Fig. 4 we present the data using wider momentum slices. The intense d band extending out to 4 au can be clearly seen. In the LMTO calculation the 3d electrons were treated as valence electrons.

The calculation, while it underestimates the binding energy of the 3d band by 4 eV, describes the ratio of the valence band to 3d intensity reasonably well.

Another feature that can be seen is that even after deconvolution a relatively intense shoulder persists on the high binding energy side of the valence band, similar to what was observed in the Auger spectra (Fig. 1). A comparison of the Auger spectra and EMS measurements at zero momentum are given below in Fig. 5. The intensity and width as obtained by the different spectroscopies is strikingly similar. The shoulder has previously been observed in the Ge KLL Auger spectrum by Berényi et al. (2004) and was attributed to shake-up from the $3d_{5/2}$ to $4d_{5/2}$ state. They had calculated that this peak should appear around 14 eV separation from the main 1D_2 peak but its intensity was calculated to be only a few % of the main line (Mukoyama et al., 1999; Cserny et al., 2000). Using EMS we observed similar satellites for Al and Si (Vos et al., 2002; Kheifets et al., 2003) as we find for Ge using both Auger and EMS spectroscopy. Al and Si do not contain d electrons. Hence we think that in all cases the satellite is due to intrinsic plasmons excited by the sudden removal of an electron.

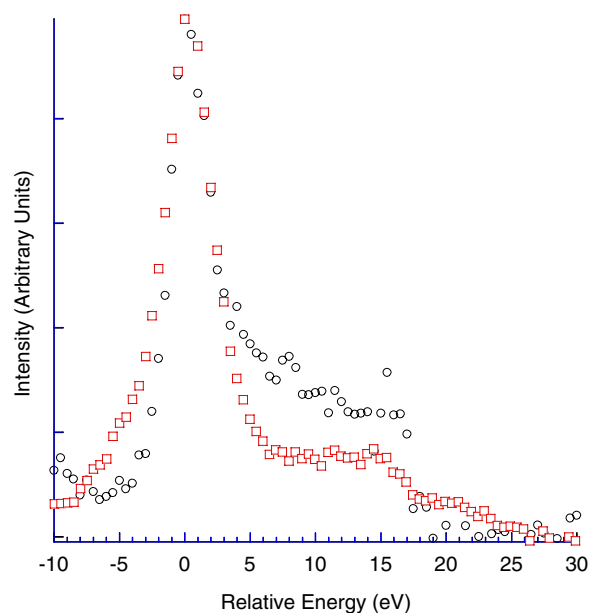


Fig. 5. Comparison of Auger and EMS measurements. The maximum intensity of the main 1D_2 Auger peak (Squares, red online) is aligned with the peak of the EMS valence band spectrum at zero momentum (circles, black online). No comparison should be made about the widths of the main valence band and Auger peak which have different origins. The similarity in the observed satellite structure in both cases indicate a common origin.

4. Summary and conclusion

The LMTO calculations we have presented are in good agreement in both position and intensity for the measured Ge valence band this agreement is expected to improve if life-time broadening is included in the theory. The calculations also accurately predict the momentum profile of the 3d band but the agreement in the calculated and observed 3d binding energy is poor.

By performing a relatively simple deconvolution procedure we have been able to separate the contributions from extrinsic and intrinsic satellites. The intrinsic satellite structure in amorphous Ge (found in both EMS and Auger spectroscopy) is similar and hence we attribute it to be due to intrinsic plasmons caused by the sudden removal of an electron.

References

- Berényi, Z., Kövér, L., Tougaard, S., Yubero, F., Tóth, J., Cserny, I., Varga, D., 2004. Contribution of intrinsic and extrinsic excitations to KLL Auger spectra induced from Ge films. *J. Electron. Spectrosc. Relat. Phenom.* 135, 177.
- Bowles, C., Went, M.R., Kheifets, A., Vos, M., 2006. Direct measurement of spectral momentum densities of single crystals using high energy EMS spectroscopy. *AIP conference proceedings*, 811, 167.
- Cserny, I., Kövér, L., Nakamatsu, H., Mukoyama, T., 2000. Solid-state effects on the satellite structure of KLL Auger spectra in Cu and Ni. *Surf. Interface Anal.* 30, 199.
- Kheifets, A.S., Sashin, V.A., Vos, M., Weigold, E., Aryasetiawan, F., 2003. Spectral properties of quasiparticles in silicon: a test of many-body theory. *Phys. Rev. B* 68 (23), 233205.
- Kovalík, A., Yakushev, E., Filosofov, D., Gorozhankin, V., Vylov, T., 2002. First experimental investigation of the KLL Auger spectrum of Ge ($Z = 32$). *J. Electron. Spectrosc. Relat. Phenom.* 123, 65.
- Kövér, L., Kovács, Z., Tóth, J., Cserny, I., Varga, D., Weightman, P., Thurgate, S., 1999. Origin of the satellites in the high resolution KLL Auger spectra of the 3d metals, Cu and Ni, and their alloys. *Surf. Sci.* 433–435, 833.
- Larkins, F.P., 1977. Semiempirical Auger-electron energies for elements $10 \leq Z \leq 100$. *At. Data Nucl. Data Tables.* 20, 311.
- Mukoyama, T., Ito, Y., Taniguchi, K., 1999. Atomic excitation and ionization as the result of inner-shell vacancy creation. *X-Ray Spectrom.* 28, 491.
- Tanuma, S., Powell, C., Penn, D., 1993. Calculations of electron inelastic mean free paths (IMFPS). IV. Evaluation of calculated IMFPS and of the predictive IMFP formula TPP-2 for electron energies between 50 and 2000 eV. *Surf. Interface Anal.* 20, 77.
- Tougaard, S., 1988. Quantitative analysis of the inelastic background in surface electron spectroscopy. *Surf. Interface Anal.* 11, 453.
- Vos, M., Cornish, G.P., Weigold, E., 2000. High-energy ($e, 2e$) spectrometer for the study of the spectral momentum density of materials. *Rev. Sci. Instr.* 71, 3831.

- Vos, M., Kheifets, A.S., Sashin, V.A., Weigold, E., Usuda, M., Aryasetiawan, F., 2002. Quantitative measurement of the spectral function of aluminum and lithium by electron momentum spectroscopy. *Phys. Rev. B.* 66 (15), 155414.
- Went, M., Vos, M., 2005. Electron-induced KLL Auger electron spectroscopy of Fe, Cu and Ge. *J. Electron Spectrosc. Relat. Phenom.* 148, 107–114.
- Zeppenfeld, K., Raether, H., 1966. Energieverluste von 50 keV-Elektronen an Ge und Si. *Z. Phys.* 471, 193.